Electric Power Systems Research 217 (2023) 109102

Contents lists available at ScienceDirect

Electric Power Systems Research

journal homepage: www.elsevier.com/locate/epsr

Current propagation type self-consistent leader-return stroke model

Vernon Cooray [a,*], Marcos Rubinstein [b], Farhad Rachidi [c]

[a] Department of Electrical Engineering, Uppsala University, 75237 Uppsala, Sweden
[b] HEIG-VD, University of Applied Sciences and Arts Western Switzerland, 1401 Yverdon-les-Bains, Switzerland
[c] Electromagnetic Compatibility Laboratory, Swiss Federal Institute of Technology (EPFL), 1015 Lausanne, Switzerland

ARTICLE INFO

Keywords:
Lightning
Return stroke
Modelling
Lightning leader
Return stroke modeles

ABSTRACT

A current propagation type return stroke model which is consistent with the estimated distribution of the charge on the leader channel is described. The model takes into account the dispersion of the return stroke current along the return stroke channel. The model is capable of generating lightning return stroke electromagnetic fields that are in close agreement with experimental observations. The model could also be used to estimate the electric fields from the leader-return stroke combination at any given distance.

1. Introduction

Engineers use return stroke models to estimate electromagnetic fields generated by lightning at different distances [1]. Return stroke models can be categorized into physics-based models, Transmission Line models, Electromagnetic models, Waveguide models, and Engineering models [1–3]. Out of these different model types, engineering models are the best suited for the calculation of electromagnetic fields due to the fact that their predictions agree reasonably well with measured electromagnetic fields. Engineering models can be divided into Current Propagation (CP), Current Generation (CG), and Current Dissipation (CD) models [1], although Current Propagation models are in fact a special case of current dissipation models and all these model types can be considered as special cases of a more general return stroke model, called the Current Model [4]. This general model can be reduced to either CP, CG or CD by a suitable selection of model parameters.

The most popular engineering models are the Modified Transmission Line (MTL) type models [5–7]. MTL type models are actually modifications of the Transmission Line Model (TL) [8]. In these models, the way in which the return stroke current amplitude decreases with height, i.e., the current attenuation function, is specified as an input parameter. In a recent paper, Cooray et al. [9] showed that the information concerning the current attenuation function in MTL type models can be extracted from the distant radiation field. They also pointed out that a necessary condition for the MTL type models to generate all the experimentally observed features of the return stroke electromagnetic fields is the inclusion of the current dispersion. Based on these considerations, they came up with an MTL type model that incorporates current dispersion and whose attenuation function is derived from the typical shape of the measured return stroke radiation fields. The model is called Modified Transmission Line Model with Derived Attenuation Function (MTLD).

The input parameters of CP models are the channel base current, the current attenuation function that describes the way in which the current is attenuated with height, the equations describing the current dispersion and the return stroke speed. The attenuation function can be converted directly into a function that describes the distribution of the charge deposited by the return stroke along the channel and vice versa [10]. Thus, the current attenuation function of MTL models can also be obtained if the distribution of the charge deposited by the return stroke (from here onwards this parameter is called return stroke charge distribution) is estimated. The goal of this paper is to develop an engineering model that belongs to the CP type with the distribution of the charge deposited by the return stroke, channel base current, and return stroke speed as input parameters. The return stroke charge distribution necessary for the model is obtained from the work conducted by Cooray et al. [11], who estimated the charge distribution along the leader channel as a function of the return stroke peak current. For this reason, the model could be used in a self-consistent manner by combining it with a down coming leader to estimate not only the return stroke fields but also the electromagnetic fields generated by the leader-return stroke combination. For this reason, the engineering model that we will develop here will be called **SLR-CP** with **SLR** standing for **S**elf consistent **L**eader-**R**eturn stroke model and **CP** standing for **C**urrent **P**ropagation.

* Corresponding author.
E-mail address: vernon.cooray@hvi.uu.se (V. Cooray).

https://doi.org/10.1016/j.epsr.2022.109102
Received 12 September 2022; Received in revised form 30 November 2022; Accepted 27 December 2022
Available online 12 January 2023
0378-7796/© 2022 The Author(s). Published by Elsevier B.V. This is an open access article under the CC BY license (http://creativecommons.org/licenses/by/4.0/).

2. SLR-CP model

In the CP models used frequently in the literature [5–8], the input parameters are the channel base current, current attenuation function with height and the return stroke speed. From these three input parameters, the measurable quantities are the channel base current and the speed of the return stroke. The current attenuation function can be either estimated from the distant radiation field [9] or from any estimation of the distribution of the charge deposited by the return stroke. However, in reference [9] it was shown that this inverse problem can give erroneous results if the current dispersion is not taken into account.

The input parameters of the SLR-CP model are the distribution of the charge neutralized by the return stroke, the channel base current, and the return stroke speed. We will utilize the leader charge distribution derived by Cooray et al. [11] to extract the distribution of the charge deposited by both first and subsequent return strokes along the leader channel (henceforth called the first return stroke charge or subsequent return stroke charge) and, from it, the current attenuation function. We will also include the current dispersion along the return stroke channel using a procedure identical to that used previously by Cooray et al. [11]. The return stroke speed is assumed to be uniform and equal to 1.0×10^8 m/s for first and 1.5×10^8 m/s for subsequent return strokes. However, it is a trivial matter to change the uniform speed to a non-uniform one.

2.1. The distribution of the charge deposited by the return stroke along the leader channel and the channel base current waveform

In a recent study, utilizing the return stroke current waveforms of downward negative lightning flashes measured by Berger [12], Cooray et al. [11] obtained the charge brought to ground by the first 100 μs of the first return stroke and the first 50 μs of the subsequent return strokes. They found a strong correlation between the peak return stroke current and the transferred charge to ground by return strokes. Combining this information with the bi-directional leader model [13] and a simplified cloud model as described in [11], they investigated how this charge was distributed along the stepped and dart leader channels. The results obtained in that study can be approximated by

$$\rho_l(\xi) = I_r\left[a_0\left(1-\frac{\xi}{H-z_0}\right)\left(1-\frac{z_0}{H}\right)+\left(1-\frac{z_0}{H}\right)\frac{(a+b\xi)}{1+c\xi+d\xi^2}\right] \quad (1)$$

In the above equation, z_0 is the vertical height of the tip of the leader, H is the total vertical length of the leader channel in meters, $\rho(\xi)$ is the charge per unit length of the leader channel located at a vertical distance ξ from the tip of the leader channel and I_r is the peak return stroke current in kA. Observe that Eq. (1) is slightly different to the one given in [11]. Eq. (1) is simpler than the one given in that reference but it generates an identical charge distribution. The geometry and relevant parameters are identified in Fig. 1a.

In the case of first return strokes, the charge per unit length of the stepped leader channel ρ_{sl} is given when $a_0 = 1.476 \times 10^{-5}$ Cm^{-1} kA^{-1}, a=4.857 × 10^{-5} Cm^{-1}kA^{-1}, b =3.909 × 10^{-6} Cm^{-2}kA^{-1}, c=0.522 m^{-1}, and d =3.73 × 10^{-3} m^{-2}. In the case of dart leaders, the charge per unit length ρ_{dl} is obtained with a_0= 5.09 × 10^{-5} Cm^{-1}kA^{-1}, a=1.325 × 10^{-6} Cm^{-1}kA^{-1}, b =7.06 × 10^{-6} Cm^{-2}kA^{-1}, c=2.089 m^{-1}, and d =1.492 × 10^{-2} m^{-2}. Observe that this equation represents the charge distribution of a leader channel of length H corresponding to a return stroke peak current with peak amplitude I_p.

Cooray [14] utilized the expression for the leader charge distribution derived by Cooray et al. [11] to estimate the distribution of charge per unit length deposited by the return stroke on the leader channel. In deriving this, he appealed to the same bidirectional leader model that was utilized by Cooray et al. [11] in estimating the leader charge distribution given above. According to the bidirectional leader model, during the return stroke process, in addition to neutralizing the negative charge (we are considering a negative return stroke here) already located on the leader channel, additional positive charge will be added along the channel [13]. According to this work, the derived charge per unit length $\rho(z)$ deposited by a return stroke as a function of the length along the channel, in which z is the position from the ground to height z along the return stroke channel, is given by

$$\rho_{ret}(z) = I_r\left\{a_0+\frac{(a+zb)}{1+cz+dz^2}\right\} \quad (2)$$

Note that in (2), the charge is expressed as a function of the height z above the ground, as opposed to (1) which is expressed as a function of distance ξ from the tip of the leader channel. The geometry and relevant parameters are identified in Fig. 1b.

In the above equation, I_r is the peak return stroke current in kA. Observe that Eqs. (1) and (2) represent the charge deposited by both first and subsequent return stroke currents. It is also important to point out that the charge distributions given by Eqs. (1) and (2) are based on static calculations and they neglect the dynamics of the charging of the leader channels. For example, consider the dart leader. At the time at which the dart leader tip reaches the ground, the dart leader current peak occurs at a height of about ten meters above the ground. This is the case because the dart leader current risetime is about 1 μs and the speed of the dart leader close to ground is about 10^7 m/s [15]. In the case of first return strokes, the initial phase of the return stroke takes place along the streamer region of the stepped leader, where the charge density could be less than that on the fully developed part of the stepped leader channel.

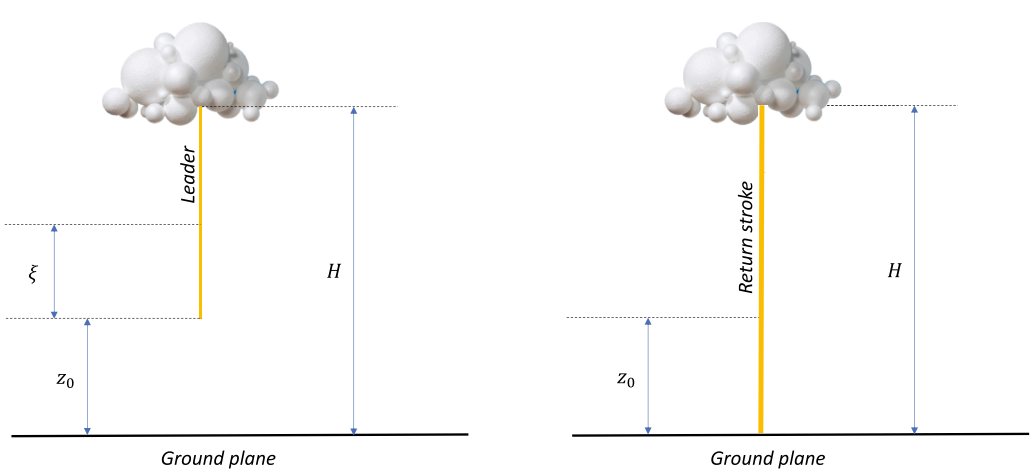

Fig. 1. Geometry and relevant parameters for the evaluation of the charge distribution along the leader channel (a) and the charge distribution deposited by the return stroke along the leader channel.

Thus, even in the case of first return strokes, one can expect the charge density to increase initially over a length roughly on the order of a step length, i.e., about 10 m [16]. In order to take these effects into account, the charge distribution is modified slightly by assuming that the peak of the distribution is reached not at ground level as in Eq. (1) but at some height. This is done simply by multiplying the charge distributions by a factor $(1 - e^{-\xi/\lambda})$. This modification gives the charge density along a fully extended leader channel as

$$\rho_l(z) = \left(1 - e^{-z/\lambda}\right) I_r \left\{ a_0 \left(1 - \frac{z}{H}\right) + \frac{(a + bz)}{1 + cz + dz^2} \right\} \tag{3}$$

The resulting charge distribution of the return stroke is

$$\rho_{ret}(z) = \left(1 - e^{-z/\lambda}\right) I_r \left\{ a_0 + \frac{(a + bz)}{1 + cz + dz^2} \right\} \tag{4}$$

Note that the expression given in Eq. (4) is the same as that in Eq. (2) except for the factor that appears outside the bracket. In our analysis, we will select λ= 10 m for both first and subsequent strokes. It is important to point out that this change in the charge distribution does not influence the results of the calculations to be presented here. Thus, for all practical purposes, one can use the charge distributions given by Eqs. (1) and (2) in the model. In a recent study, the same charge distribution was used in [17] to construct a CG type return stroke model which could predict the effect of the local ground conductivity at the strike point on the return stroke current parameters.

The charge distributed by the first and subsequent return strokes as given by Eq. (4) are depicted in Fig. 2. Note that the charge deposited by the return stroke increases initially with height, reaches a peak and then decreases rapidly with height approaching a constant value for heights larger than about 1 km.

Consider a return stroke channel of height H. The total charge, Q, deposited along the channel by the return stroke is given by

$$Q = \int_0^H \rho(\zeta) d\zeta \tag{5}$$

If we assume that the current at the upper channel end is zero (boundary condition), then this charge should be equal to the total charge contained in the channel-base current, $I_b(t)$. That is

$$Q = \int_0^H \rho(\zeta) d\zeta = \int_0^\infty I_b(t) dt \tag{6}$$

This shows that for a given channel-base current with a specified peak current, there is a specific channel length that accommodates its charge or vice versa. For example, the total charge available for a first return stroke current of 30 kA is 1.89 C, 2.34 C, or 2.79 C respectively for 4 km, 5 km and 6 km long channels. Similarly, for a subsequent stroke of 12 kA, the corresponding charges are 0.26 C, 0.33 C, and 0.39 C. This means the channel length and the channel-base current cannot be freely specified because both parameters depend on each other. In the model, we can select the channel-base current waveform and fit the height of the channel to the selected current waveform or we can select the channel height and fit the duration of the current waveform to match the resulting charge. In this paper, we have decided to select the channel height as the independent parameter. A discussion on this point is given in Section 4.

In the calculations to be presented here, we will utilize a channel height of 6 km for both first and subsequent strokes. This will fix the charge associated with the channel-base current waveform. There are several standard current waveforms available to represent first and subsequent strokes. The charge associated with them can be changed by changing the decay time constant of the current waveform. The first return stroke current waveform based on Heidler's functions is given by [18]

$$i(t) = i_{01} \frac{(t/\tau_{11})^2}{(t/\tau_{11})^2 + 1} e^{-t/\tau_{12}} \tag{7}$$

with i_{01} = 30.57 kA, τ_{11} = 0.09 μs andτ_{12} = 92.0 μs. The channel-base current of the subsequent return stroke is given by

$$i(t) = i_{01} \frac{(t/\tau_{11})^2}{(t/\tau_{11})^2 + 1} e^{-t/\tau_{12}} + i_{02} \frac{(t/\tau_{21})^2}{(t/\tau_{21})^2 + 1} e^{-t/\tau_{22}} \tag{8}$$

with the parameters i_{01} = 13.751 kA, i_{02} = 9.252 kA, τ_{11} = 0.055 μs, τ_{12} = 2.0 μs, τ_{21} = 2.0 μs, and τ_{22} = 41.6 μs. These are similar to the typical current waveforms used in the literature except in the case of subsequent strokes which has somewhat smaller duration than the ones used in practice. Both these current waveforms dissipate all their charge along

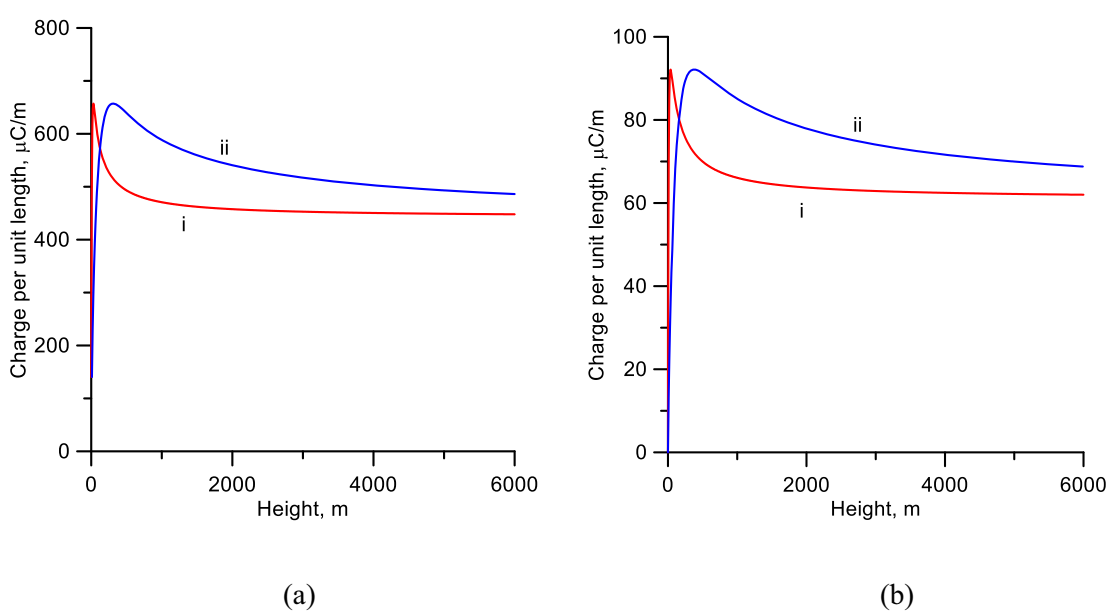

Fig. 2. The charge deposited by (a) a 30-kA-peak first return stroke (curve i) and by (b) a 12-kA-peak subsequent return stroke (curve i) along the leader channel. The curves marked ii show the charge distribution over the first 600 m on 10 times longer length scale.

the 6 km long channel and the current amplitude at the channel end goes to zero. With the selected parameters, the net charge transported up by these two currents are the values given above, 2.8 C and 0.39 C, respectively. These current waveforms are depicted in Fig. 3.

2.2. Current attenuation function

Once the charge deposited by the return stroke as a function of height is known, one can convert it directly to the current attenuation function in the current propagation type return stroke models. The relationship between the attenuation function and the charge deposited per unit length by the return stroke at any given height is given by [10]

$$\rho(\zeta) = -\frac{\partial A(\zeta)}{\partial \zeta} Q \tag{9}$$

Note that this equation is valid for a dispersion-free propagation. It is also valid when the dispersion function itself does not lead to charge deposition along the channel.

In the above Equation$\rho(\zeta)$ is the charge dissipated by the return stroke per unit length, A is the current attenuation function, ζ is the length along the channel and Q is the total charge dissipated by the return stroke along the channel. Knowing the channel-base current waveform, one can estimate the current attenuation function from the above equation. The attenuation function extracted for the first return stroke and the subsequent return strokes are shown by solid lines marked '1′ in Fig. 4a and b. The attenuation function can be closely approximated by the function

$$A(\zeta) = 1 - \frac{\zeta}{L_c} \tag{10}$$

where L_c is the total length of the channel. We have used the subscript c to indicate that one cannot freely select this length but it is directly coupled to the total charge dissipated by the return stroke. This is also plotted in Fig. 4a and b by the lines marked '2′.

It is important to point out that a linearly decreasing attenuation function corresponds to a constant charge deposition along the leader channel by the return stroke. However, the return stroke charge distributions shown in Fig. 2 deviate significantly from a constant charge distribution at small heights. Thus, even though the curves '1′ and '2′ in Fig. 4 appear almost the same, they have enough differences to affect the finer details of the return stroke field.

2.3. Current dispersion

As shown recently by Cooray et al. [9], in order to generate results in agreement with experiment, in addition to current attenuation, the return stroke current in the CP type models should undergo dispersion as it propagates along the channel. In reference [9], the presence of current dispersion is introduced into return stroke models by an expression for the dispersion of an impulse current as it propagates along the channel. We will use the same expression here. The expression used to represent the dispersion of an impulse as a function of the length z measured along the channel is given by

$$R_\delta(t,z) = \frac{e^{-t/t_r(z)}}{t_r(z)} \tag{11}$$

The parameter $t_r(z)$, which is a measure of the width of the response function, is given by

$$t_r(z) = t_0\left(1 - e^{-z^2/\lambda_r^2}\right) \tag{12}$$

Note that Eq. (11) reduces to an impulse function at ground level and its width increases with increasing height. Note that λ_r is a constant that defines how the width of the response function changes with height. Observe that the time integral of $R_\delta(t,z)$ is equal to unity, a necessary criterion to ensure that there is no charge deposition along the channel as the current disperses.

This dispersion formula also shows that a step current pulse at ground level will change with height according to the expression

$$R_H(t,z) = 1 - e^{-t/t_r(\zeta)} \tag{13}$$

Observe that the risetime of the step current pulse increases initially but it will be clamped to a fixed value as the height increases beyond about λ_r. As we will show later, this clamping of the risetime is a necessary feature in the current dispersion to generate a subsidiary peak in the distant radiation field which is observed frequently in the radiation fields of subsequent return strokes. Once the response function for a step current is given, the effect of dispersion on any other current waveform can be obtained using the Duhammel's theorem. It is important to point out that current dispersion is a feature that is always present in actual return strokes, as demonstrated by Jordan and Uman [19] and Mack and Rust [20] using optical observations. These measurements indicate that the optical risetime may increase by about a microsecond or so in travelling about 1 km of the channel. However,

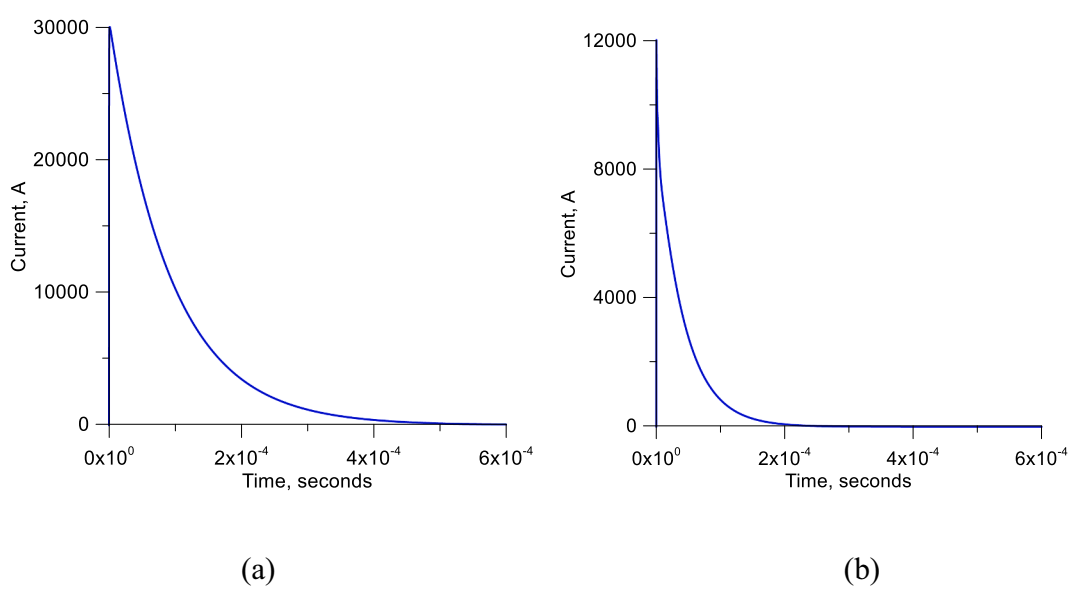

Fig. 3. The channel base current in (a) first and (b) subsequent return stroke.

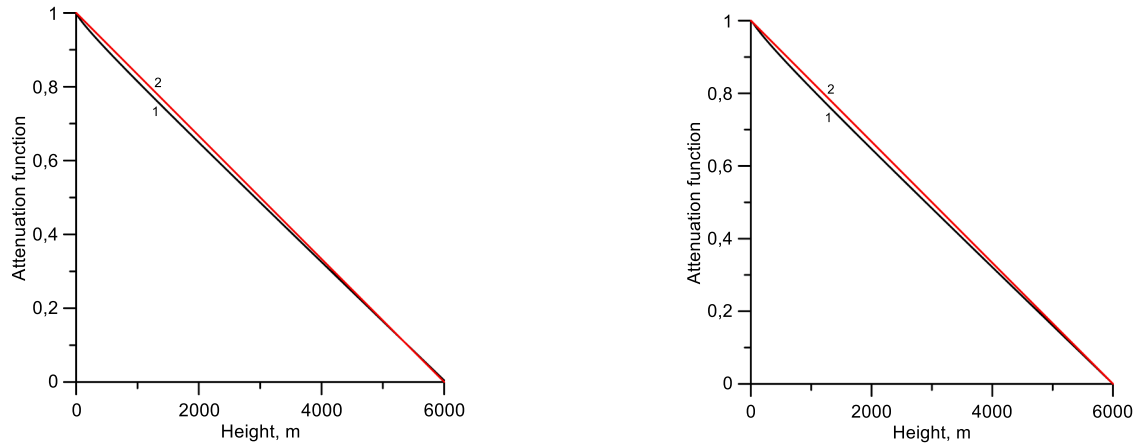

Fig. 4. The current attenuation function of (a) first return strokes and (b) subsequent return stroke. The current attenuation functions derived from the charge distribution given by Eq. (4) are denoted by the curves marked '1′ and the linear approximation for the charge distributions (Eq. (10)) are shown by the curves marked 2.

experimental data also show that the optical radiation may not follow the rising part of the current waveform exactly; the risetime of the current being somewhat smaller than the optical radiation [21,22]. Thus, optical radiation provides evidence for the presence of current dispersion, and hence the need to incorporate it into return stroke models, but it does not provide quantitative information on the effect of current dispersion on the risetime of the current.

We have now defined all the parameters necessary for the SLR-CP model. In the following section we will present the results pertinent to the SLR-CP model. In all the presented calculations, the ground is assumed to be perfectly conducting.

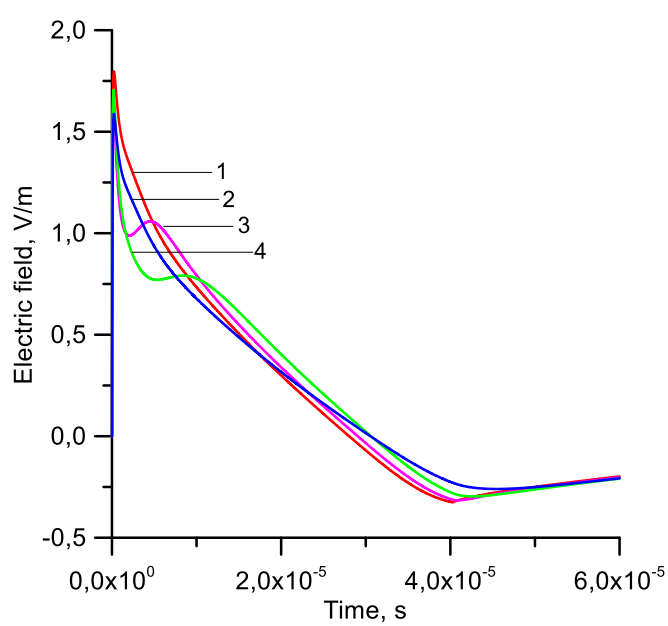

Fig. 5. The effect of dispersion of the current on the radiation fields of subsequent return strokes. The radiation field is calculated at 200 km distance. Curve 1: Without dispersion. Curve 2:$t_r(z) = 10^{-6}z/1000.0$. Curve 3: $t_0 = 1.0 \times 10^{-6}$ s and λ_r=250.0 m. Curve 4: $t_0 = 2.5 \times 10^{-6}$ s and λ_r=500.0 m. In these equations, z is the height along the return stroke channel.

3. Derived features of the SLR-CP model

3.1. Effect of current dispersion

The radiation fields of a subsequent return stroke at 200 km for different dispersion functions are shown in Fig. 5. Note that the dispersion will introduce a subsidiary peak in the radiation field. However, if the dispersion is such that the risetime of the current increases monotonically, the subsidiary peak of the electric field disappears. The broadness of this subsidiary peak is determined by t_0 and λ_r. In the rest of the calculations, we will use $t_0 = 1.0 \times 10^{-6}$ s and λ_r=250.0 m for both first and subsequent return strokes (corresponding to curve 3 in Fig. 4). These are the parameters used by Cooray et al. [9] in the MTLD model.

3.2. Variation of return stroke current with height

The return stroke current as a function of height for both first and subsequent return strokes is shown in Fig. 6. Observe that the initial part of the current attenuates with height. At the same time, due to dispersion, its risetime will increase initially, but then it will become steady with height.

3.3. Electric field at different distances

The electric and magnetic fields calculated at different distances incorporating the current dispersion are shown in Figs. 7–10 for first and subsequent return strokes. Note that the model can reproduce the main features of the return stroke electromagnetic fields observed in experimental data [23,24]. Specifically, compared to the experimentally derived typical electric field waveforms in Fig. 1 of [23], the features that are reproduced by our model are the ramp at distances below 10 km, the initial peak after 5 km followed by a distinctive start of the electric field ramp, and the zero-crossing time at 40 to 50 μs for distances greater than 50 km. For the magnetic field, the features reproduced are the hump at distances lower then 15 km, the initial peak at distances greater than 2 km, and the zero-crossing time at 40 to 50 μs for distances greater than 50 km.

According to experimental data, the electric field at 50 m of subsequent return strokes saturates within a few microseconds. This is a feature observed in the subsequent strokes of triggered lightning. Whether the same feature should be present in first return strokes needs further observations. Moreover, the tail of the electric field at around 1 to 5 km shows a ramp-like increase, and the corresponding magnetic fields display a prominent hump. Furthermore, the radiation fields cross

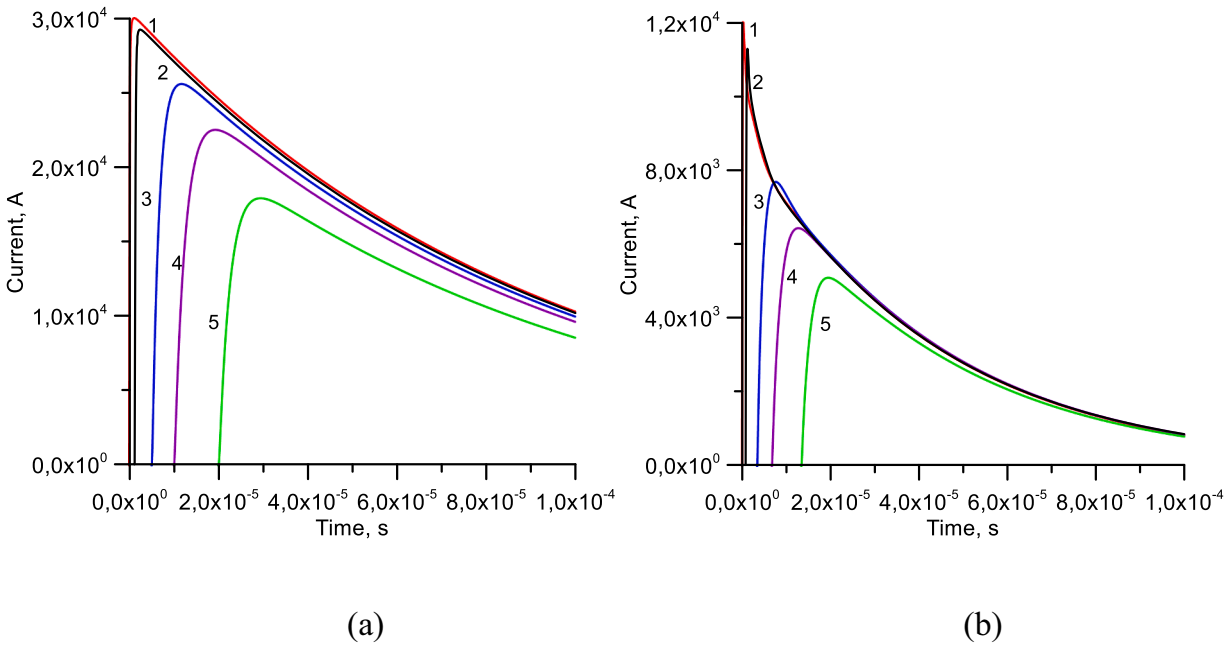

Fig. 6. The current at different heights in (a) first return strokes and (b) subsequent return strokes. Curve 1: 0 m, Curve 2: 100 m, Curve 3: 500 m, Curve 4: 1000 m, Curve 5: 2000 m.

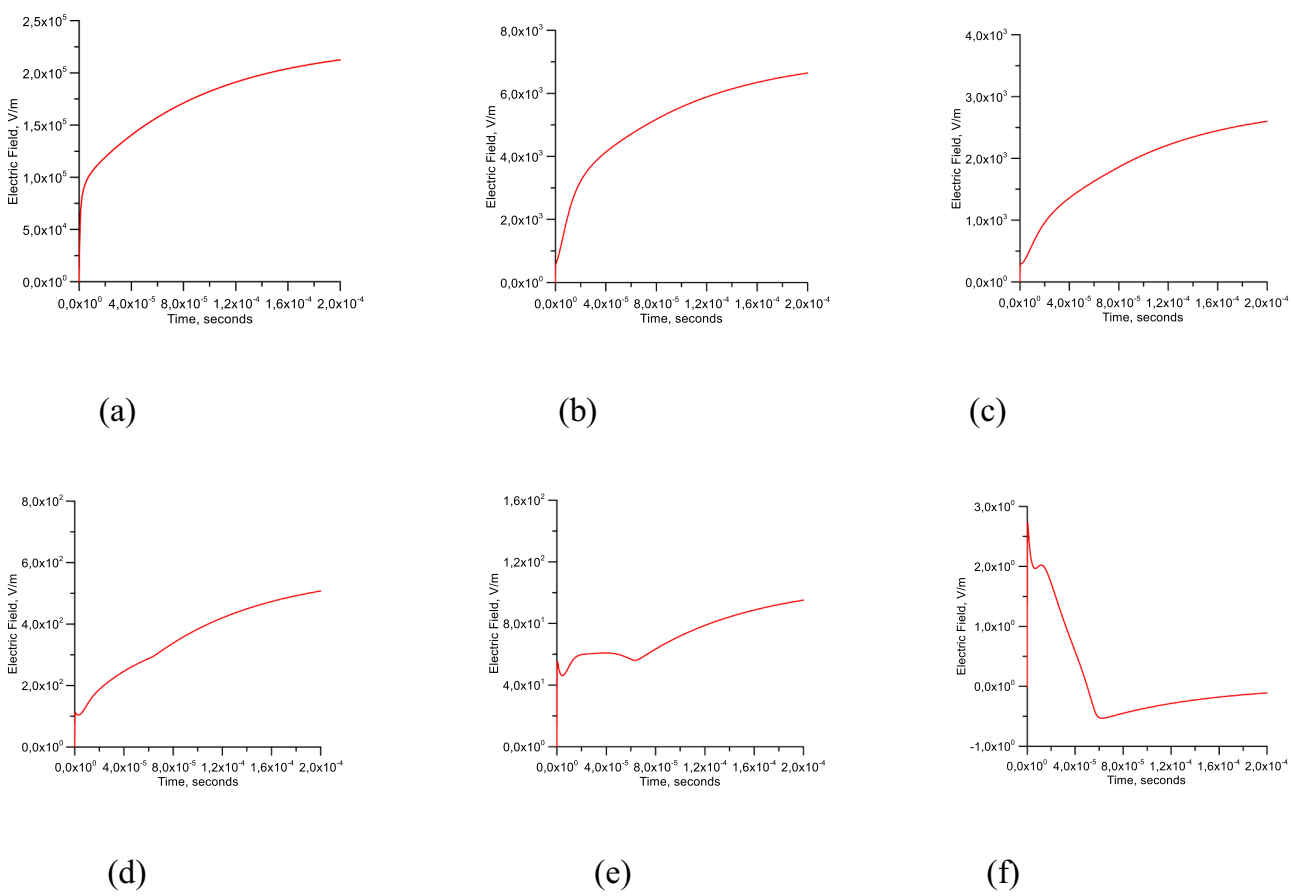

Fig. 7. Electric fields generated by first return strokes over the distance range from 50 m to 200 km. (a) Electric field at 50 m, (b) Electric field at 1 km, (c) Electric field at 2 km, (d) Electric field at 5 km, (e) Electric field at 10 km, (f) Electric field at 200 km.

the zero line and display the characteristic subsidiary peak. The peak value of the radiation field at 100 km is 3.4 V/m for subsequent return strokes and 5.5 V/m for first strokes. These values do not differ significantly from the TL model. This is the case because the change in current amplitude and shape with height due to attenuation and dispersion does not affect significantly the peak value of the current over

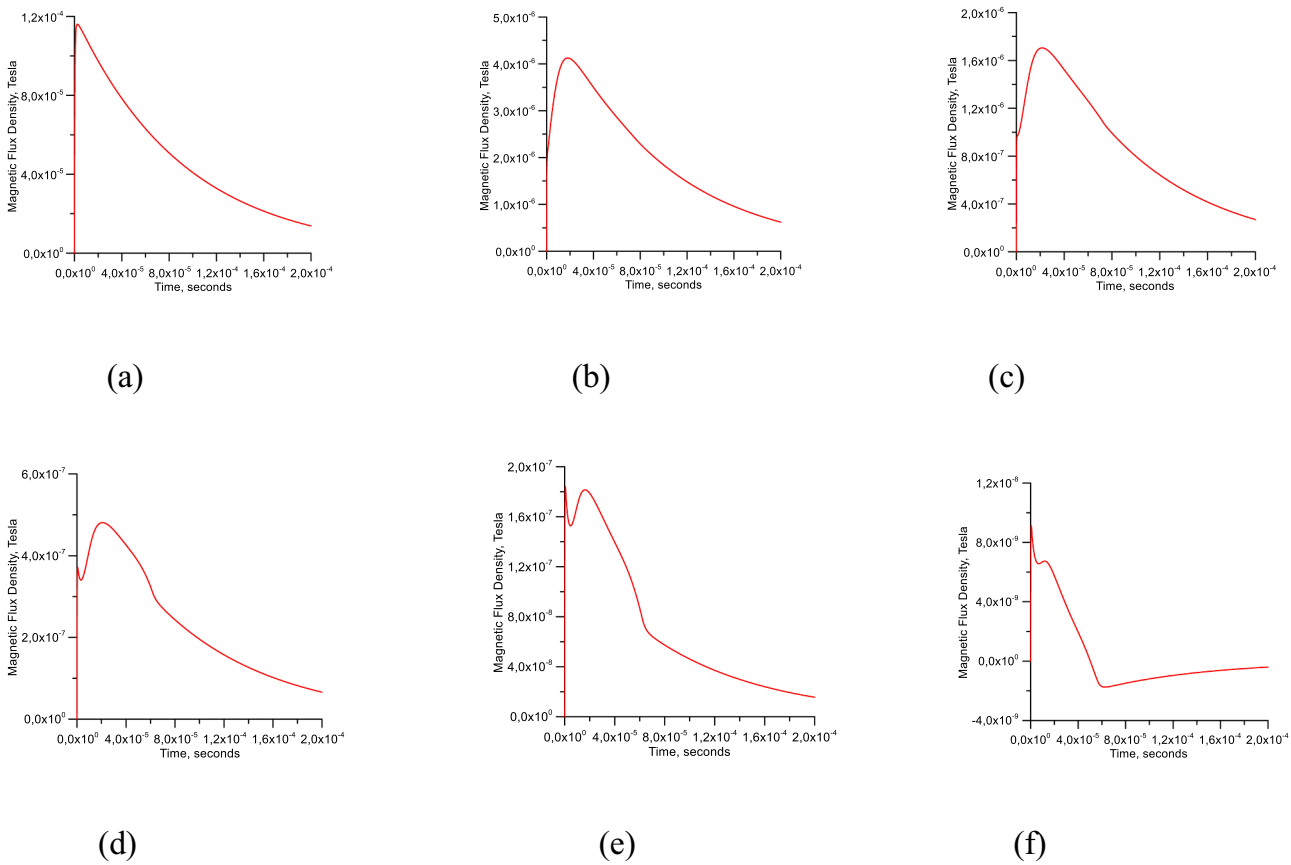

Fig. 8. Magnetic fields generated by first return strokes over the distance range from 50 m to 200 km. (a) Magnetic field at 50 m, (b) Magnetic field at 1 km, (c) Magnetic field at 2 km, (d) Magnetic field at 5 km, (e) Magnetic field at 10 km, (f) Magnetic field at 200 km.

the first few tens of meters. These features show that even though the introduction of current dispersion makes the model slightly more complex, it compensates for this by generating electromagnetic fields with features in good agreement with experimental observations. Note that the sudden change apparent in the electromagnetic fields, especially the first return stroke fields pertinent to 10 km distance, is actually caused by the sudden termination of the return stroke channel at 6 km height. These changes will be smoothed out considerably if one considers a return stroke speed that decreases along the channel.

The magnetic field at 50 m resembles mostly the channel base current and it is similar to the experimental data. The magnetic field at intermediate distances displays the characteristic hump. The distant magnetic field being mainly radiation, it has the same features as those of the electric radiation field.

3.4. Electromagnetic radiation field derivative

The derivatives of the radiation field produced by the first and subsequent strokes are shown in Fig. 11. The range normalized peak field derivative of first return strokes is 43 V/m/μs and the one corresponding to the subsequent strokes is 48 V/m/μs. These values are in general agreement with experimental observations [25]. The full width at half maximum of the electric field derivative is about 50 −100 ns, which is also in agreement with experimental observations. Of course, for a given return stroke speed, the peak value of the electric field derivative at any given distance is controlled to some extent by the derivative of the channel-base current waveform used as an input.

3.5. Leader-return stroke fields

In this paper, we have introduced a model which belongs to the CP category. The main difference compared to other models is the use of the dart leader charge distribution as the basic input. One advantage of the model is the following. The leader charge distribution derived by Cooray et al. [11] has been used frequently in estimating the electric field generated by down coming dart leaders. The resulting fields from the charge distribution are also in agreement with the measured dart leader fields. Since the model developed in this paper is based on this leader charge distribution, this model in combination with the dart leader model could be used in a self-consistent manner to model the leader-return stroke fields at different distances. Eqs. (1) and (3) give the variation of the leader charge as the leader descends, allowing the total field at any given point to be calculated. Fig. 12 depicts the leader return stroke field at 50 and 100 m for subsequent strokes. The general features of the dart leader-return stroke sequence are in general agreement with the experimental data obtained from triggered lightning experiments [26,27].

In the current model, since positive charge deposited along the dart leader channel after the neutralization of the negative charge close to ground is zero, the leader field is completely neutralized by the return stroke field in the vicinity of the strike point. However, as the distance to the strike point becomes longer, the effect of the positive charge deposited by the return stroke at higher points becomes effective and the return stroke field amplitude overwhelms the dart leader field. It is important to point out that in the experimental observations, sometimes the return stroke field is larger than the leader field and, in other instances, it is smaller. This observation cannot be explained within the confines of the present model. However, we would like to point out that a return stoke model that uses the same charge distribution given here but that belongs to the CG category can account for such features by introducing current reflection at ground level.

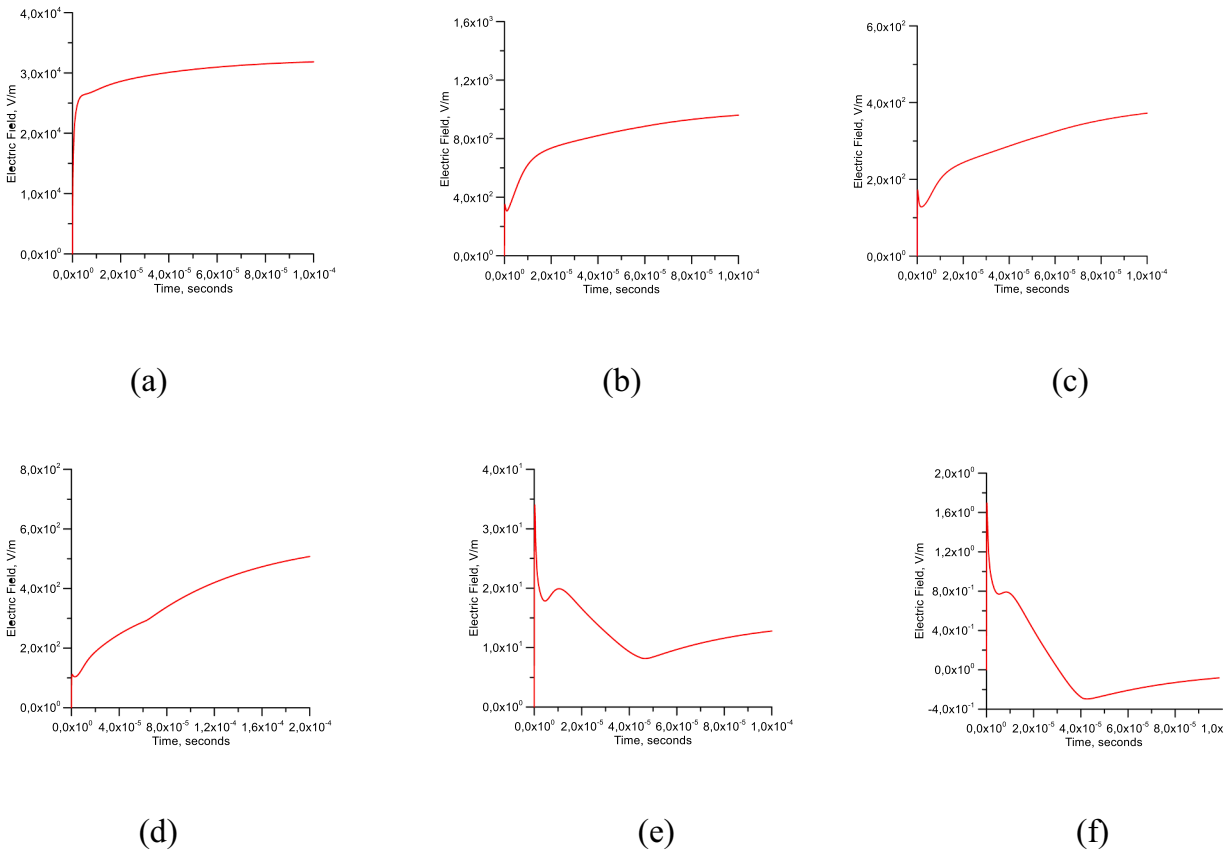

Fig. 9. Electric fields generated by subsequent return strokes over the distance range from 50 m to 200 km. (a) Electric field at 50 m, (b) Electric field at 1 km, (c) Electric field at 2 km, (d) Electric field at 5 km, (e) Electric field at 10 km, (f) Electric field at 200 km.

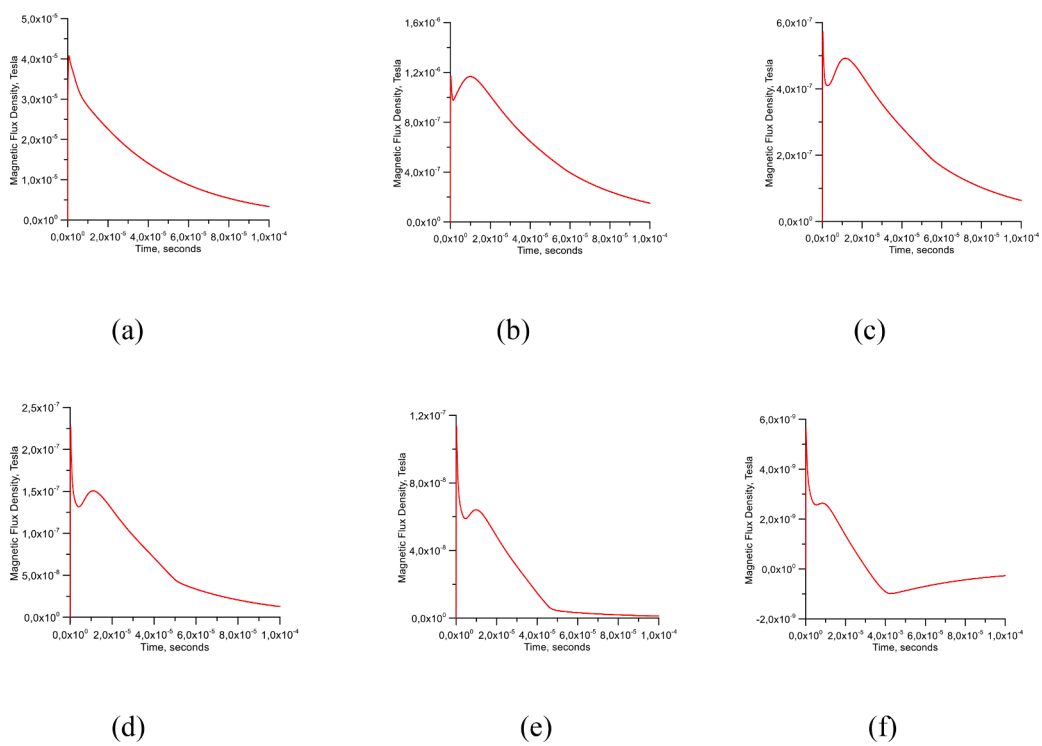

Fig. 10. Magnetic fields generated by subsequent return strokes over the distance range from 50 m to 200 km. (a) Magnetic field at 50 m, (b) Magnetic field at 1 km, (c) Magnetic field at 2 km, (d) Magnetic field at 5 km, (e) Magnetic field at 10 km, (f) Magnetic field at 200 km.

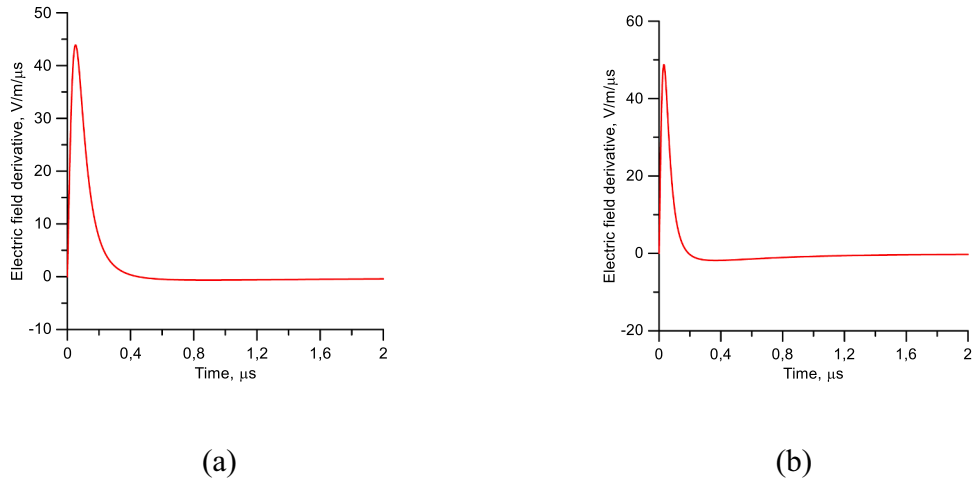

Fig. 11. Electric field derivative at 100 km generated by (a) a first return stroke and (2) a subsequent return stroke.

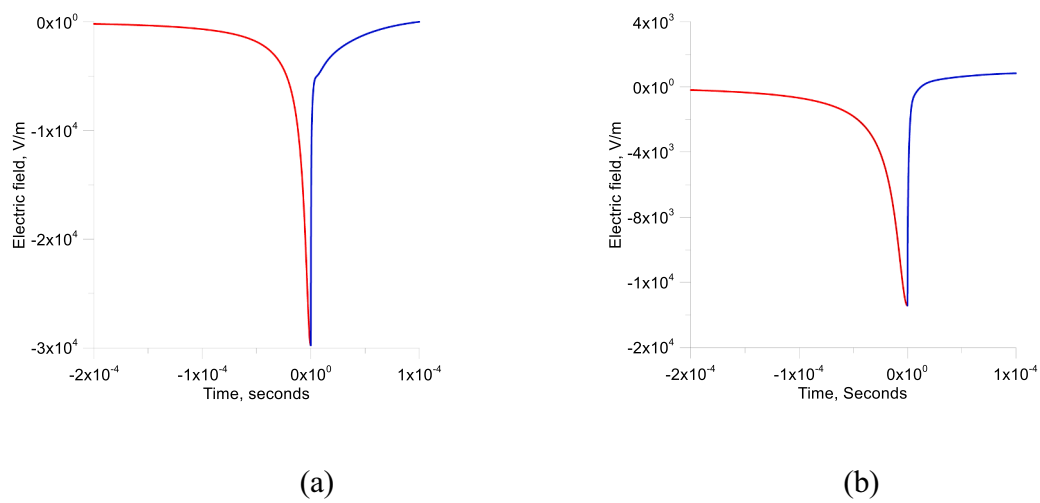

Fig. 12. The electric field generated by the dart leader- return stroke sequence at (a) 50 m and (b) 100 m. The portion of the field taking place before the zero time mark (in red) is due to the dart leader and the section of the field after the zero time mark (in blue) is due to the return stroke. The time axis is selected in such a way that the dart leader contacts the ground at the time marked zero.

4. Discussion

Experimental data show that the charge dissipated by subsequent return strokes is close to 1 C and that of first return strokes is about 4 C. These numbers are significantly larger than the charge associated with the two current waveforms used in the paper. There are two ways to accommodate a current with charge similar to that of measured currents. The first is to assume that only the first few tens of microseconds of the return stroke current injected at the channel base will contribute to the charge deposition along the channel. In this case, the tail part of the current travels along the return stroke channel without attenuation, thus without contributing to the charge deposition. This can be realized in practice by incorporating into the model a current waveform with a smaller amplitude, longer risetime, and longer duration that travels along the channel without attenuating (i.e., classical TL model). Such a scenario will make it possible to accommodate a current waveform carrying larger charge in the return stroke model. The second procedure is to consider a longer but non vertical channel. Experimental data show that return stroke channels are much longer than their vertical extent and contain large horizontal channels. By employing a long but non-vertical channel, the model will be able to accommodate a return stroke current waveform containing larger charge. Furthermore, in the model we have assumed a straight vertical channel without any branches. Extension of the model to include branches and horizontal channel sections requires information concerning the charge distribution on non-vertical channels. This requires modification of Eqs. (1) to (4) to include non-vertical channels and branches. Moreover, how to include the effects of branches in CP-type return stroke models has not yet been investigated in the literature. These points are under investigation at present.

5. Conclusions

In this paper we have described an engineering return stroke model that belongs to the CP type. The input parameters of the model are the distribution of the charge deposited by the return stroke, the return stroke speed, and the channel-base current. The charge deposited by the return stroke on the leader channel is obtained from the leader charge distribution and, for this reason, it could be used to model self consistently the leader-return stroke fields. The model incorporates current dispersion. The results obtained from the model are in reasonable agreement with experiments.

Author credit statement

All authors have read and agreed to the published version of the

manuscript.

CRediT authorship contribution statement

Vernon Cooray: Conceptualization, Methodology, Validation, Writing – original draft, Writing – review & editing. **Marcos Rubinstein:** Validation, Writing – review & editing. **Farhad Rachidi:** Validation, Writing – review & editing.

Declaration of Competing Interest

The authors declare that they have no known competing financial interests or personal relationships that could have appeared to influence the work reported in this paper.

Data availability

No data was used for the research described in the article.

References

[1] V. Cooray, Return stroke models for engineering applications, in: V. Cooray (Ed.), Lightning Protection, Published by Institute of Engineering and Technology, London, UK, 2010.

[2] V.A. Rakov, M.A. Uman, Review and evaluation of lightning return stroke models including some aspects of their application, in *IEEE Trans. Electromagn. Compatib.* 40 (4) (1998) 403–426, https://doi.org/10.1109/15.736202. Nov.

[3] C. Gomes, V. Cooray, Concepts of lightning return stroke models, IEEE Trans. Electromagn. Compatib. 42 (1) (2000). Febr.

[4] V. Cooray, Unification of engineering return stroke models, Electr. Power Syst. Res. 195 (2021), 107118.

[5] Nucci, C.A., C. Mazzetti, F. Rachidi and M. Ianoz, On lightning return stroke models for LEMP calculations," in 19th Int. Conf. Lightning Protection, Graz, Austria, 1988.

[6] Rakov, V.A. and Dulzon, A.A., A modified transmission line model for lightning return stroke field calculation," in Proc. 9th Int. Symp. Electromagn. Compat., Zurich, Switzerland, 44H1, pp. 229–235, 1991.

[7] V. Cooray, R.E. Orville, The effects of variation of current amplitude, current risetime and return stroke velocity along the return stroke channel on the electromagnetic fields generated by return strokes, J. Geophys. Res. 95 (D11) (1990). Oct.

[8] M.A. Uman, D.K. McLain, Magnetic field of lightning return stroke, J. Geophys. Res. 74 (1969) 6899–6910.

[9] V. Cooray, M. Rubinstein, F. Rachidi, Modified transmission line model with a current attenuation function derived from the lightning radiation field—MTLD model, Atmosphere (Basel) 12 (2021) 249, https://doi.org/10.3390/atmos12020249.

[10] G. Maslowski, V.A. Rakov, Equivalency of lightning return stroke models employing lumped and distributed current sources, Trans. IEEE (EMC) (49) (2007) 123–132.

[11] V. Cooray, V. Rakov, N. Theethayi, The lightning striking distance – revisited, J Electrostat 65 (5–6) (2007) 296–306.

[12] K. Berger, Novel observations of lightning discharges: results of research on Mount San Salvatore, J. Franklin Inst. 283 (1967) 478–525.

[13] H.W. Kasemir, A contribution to the electrostatic theory of a lightning discharge, J. Geophys. Res. 65 (1960) 1873–1878, https://doi.org/10.1029/JZ065i007p01873.

[14] V. Cooray, Introduction to Lightning, Springer, Heidelberg, Germany, 2015.

[15] Cooray, V.; Idone, V.P.; Orville, R.E. Velocity of a self propagating discharge as a function of current parameters with special attention to return strokes and dart leaders. In Proceedings of the International Conference on Lightning and Static Electricity, Bath, UK, pp. 14.3.1–14.3.9, 28 September 1989.

[16] C.J. Biagi, M.A. Uman, J.D. Hill, D.M. Jordan, V.A. Rakov, J. Dwyer, Observations of stepping mechanisms in a rocket-and-wire triggered lightning flash, J. Geophys. Res. Atmos. 115 (2010) D23215.

[17] V. Cooray, M. Rubinstein, F. Rachidi, A Self-Consistent Return Stroke Model That Includes the Effect of the Ground Conductivity at the Strike Point, Atmosphere (Basel) 13 (2022) 593, https://doi.org/10.3390/atmos13040593.

[18] F. Delfino, R. Procopio, M. Rossi, F. Rachidi, C.A. Nucci, An algorithm for the exact evaluation of the underground lightning electromagnetic fields, IEEE Trans. (EMC) 49 (2007) 401–411.

[19] D.M. Jordan, M.A. Uman, Variation in light intensity with and time from subsequent lightning return strokes, J. Geophys. Res. 88 (1983) 6555–6562.

[20] D.M. Mach, W.D. Rust, Photoelectric return stroke velocity and peak current estimates in natural and triggered lightning, J. Geophys. Res. 94 (1989) 13237–13247.

[21] F.L. Carvalho, D.M. Jordan, M.A. Uman, T. Ngin, W.R. Gamerota, J.T. Pilkey, Simultaneously measured lightning return stroke channel-base current and luminosity, Geophys. Res. Lett. 41 (2014) 7799–7805, https://doi.org/10.1002/2014GL062190.

[22] C. Gomes, V. Cooray, Correlation between the optical signatures and current wave forms of long sparks: applications in lightning research, J. Electrostat. 43 (4) (1998) 267–274.

[23] Y.T. Lin, M.A. Uman, J.A. Tiller, R.D. Brantley, W.H. Beasley, E.P. Krider, C. D. Weidman, Characterization of lightning return stroke electric and magnetic fields from simultaneous two-station measurements, J. Geophys. Res. 84 (1979) 6307–6314.

[24] V. Rakov, M.A. Uman, K. Rambo, A review of ten years of triggered-lightning experiments at Camp Blanding, Florida, Atmos. Res. 76 (2005) 503–517, https://doi.org/10.1016/j.atmosres.2004.11.028.18.

[25] J. Willett, E. Krider, C. Leteinturier, Submicrosecond field variations during the onset of first return strokes in cloud-to-ground lightning, J. Geophys. Res. 103 (1996) 9027–9034.

[26] V.A. Rakov, V. Kodali, D.E. Crawford, J. Schoene, M.A. Uman, K.J. Rambo, G. H. Schnetzer, Close electric field signatures of dart leader/return stroke sequences in rocket-triggered lightning showing residual fields, J. Geophys. Res. 110 (2005) D07205, https://doi.org/10.1029/2004JD005417.

[27] M. Rubinstein, F. Rachidi, M.A. Uman, R. Thottappillil, V.A. Rakov, C.A. Nucci, Characterization of vertical electric fields 500m and 30m from triggered lightning", J. Geophys. Res. 100 (D5) (1995) 8863–8872. May.